Title: Brain mechanisms for perceiving illusory lines in humans

Authors: Jacques Anken, Ruxandra I. Tivadar, Jean-François Knebel, Micah M. Murray

Journal: NeuroImage

Year: 2018

DOI: 10.1016/ j.neuroimage.2018.07.017

Brain mechanisms for perceiving illusory lines in humans

Jacques Anken[1,†], Ruxandra I. Tivadar[1,2,†], Jean-François Knebel[1,3], Micah M. Murray[1-4,*]

[1]The LINE (Laboratory for Investigative Neurophysiology), Department of Radiology and Department of Clinical Neurosciences, University Hospital Center and University of Lausanne, Lausanne, Switzerland
[2]Department of Ophthalmology, University of Lausanne, Jules-Gonin Eye Hospital, Lausanne, Switzerland
[3]Electroencephalography Brain Mapping Core, Center for Biomedical Imaging (CIBM) of Lausanne and Geneva, Switzerland
[4]Department of Hearing and Speech Sciences, Vanderbilt University, Nashville, TN, USA

[†]These authors made equal contributions.

***Address correspondence to:**
Prof. Micah Murray
CHUV-UNIL
Radiologie, BH08.078
Rue du Bugnon 46
1011 Lausanne
Micah.murray@chuv.ch

Abstract

Illusory contours (ICs) are perceptions of visual borders despite absent contrast gradients. The psychophysical and neurobiological mechanisms of IC processes have been studied across species and diverse brain imaging/mapping techniques. Nonetheless, debate continues regarding whether IC sensitivity results from a (presumably) feedforward process within low-level visual cortices (V1/V2) or instead are processed first within higher-order brain regions, such as lateral occipital cortices (LOC). Studies in animal models, which generally favour a feedforward mechanism within V1/V2, have typically involved stimuli inducing IC lines. By contrast, studies in humans generally favour a mechanism where IC sensitivity is mediated by LOC and have typically involved stimuli inducing IC forms or shapes. Thus, the particular stimulus features used may strongly contribute to the model of IC sensitivity supported. To address this, we recorded visual evoked potentials (VEPs) while presenting human observers with an array of 10 inducers within the central 5°, two of which could be oriented to induce an IC line on a given trial. VEPs were analysed using an electrical neuroimaging framework. Sensitivity to the presence vs. absence of centrally-presented IC lines was first apparent at ~200ms post-stimulus onset and was evident as topographic differences across conditions. We ~~also~~ localized these differences to the LOC. The timing and localization of these effects are consistent with a model of IC sensitivity commencing within higher-level visual cortices. We propose that prior observations of effects within lower-tier cortices (V1/V2) are the result of feedback from IC sensitivity that originates instead within higher-tier cortices (LOC).

Key words: illusory contour, Kanizsa, event-related potential (ERP), visual evoked potential (VEP).

1. Introduction

Visual boundaries are perceived even when input to the retina is discontinuous or incomplete, such as under low luminance or low contrast. These perceptions of boundaries have been investigated extensively with illusory contours (IC) (Murray and Herrmann, 2013)**.** A particular type of IC was popularized by Gaetano Kanizsa and is still widely used to investigate both the psychophysical and neurobiological bases of IC perception (Kanizsa, 1976). Kanizsa-type ICs are based on an array of circles, each of which has a sector removed (hereafter referred to as pacmen inducers). These pacmen inducers can be oriented to form an IC or rotated to block such perceptions (i.e. forming non-contours; NCs) (**Figure 1a**). Typical Kanizsa-type ICs result in the perception of geometric shapes (triangles, squares, circles, pentagons, etc.; cf. Figure 1 in(Murray et al., 2002).

Several neurophysiologic models of IC processing have been hypothesized that differ principally in terms of where (and when) sensitivity to ICs first manifests (Murray and Herrmann, 2013). One model proposes that low-level visual areas V1/V2 are sensitive to ICs in a bottom-up and feed-forward manner. Support for this model derives principally from microelectrode recordings in animals, where the IC was induced either with phase-shifted line gratings (Grosof et al., 1993; Nieder and Wagner, 1999; Redies et al., 1986; von der Heydt et al., 1984)) or with notch stimuli akin to Kanizsa-type stimuli (von der Heydt et al., 1984; Peterhans and von der Heydt, 1989) (**Figure 1b-c**). In the case of phase-shifted gratings, the line spacing and size of the receptive fields of the recorded neurons varied (e.g. 80 arcmin period and stimulus size of ~3-3.5° in Grosof et al. (1993); 0.4-12° stimuli with neurons having receptive fields ranging from 2-16° in Redies et al., (1986). In the case of the notch stimuli, the ICs were typically line segments extending just beyond the limits of the classical receptive field of the recorded neuron, spanning ~2-3° of visual angle (von der Heydt and Peterhans, 1989; Peterhans and von der Heydt, 1989).

A second model proposes that IC sensitivity is instead first achieved within lateral occipital cortices (LOC) in the ventral visual pathway (Ungerleider and Mishkin, 1982). Any effects in V1/V2

result from feedback modulations from the LOC (Anken et al., 2016; Halgren et al., 2003; Lee and Nguyen, 2001; Mendola et al., 1999; Murray et al., 2006, 2004, 2002; Poscoliero and Girelli, 2017; Sáry et al., 2008, 2007). Support for this model comes largely from studies in humans that involved IC shapes like that in Figure 1a (cf. Figure 3 in Murray and Herrmann, 2013 for a schematic summary of results across studies). In particular, our laboratory has previously identified a visual evoked potential (VEP) correlate of illusory contour sensitivity. This so-called IC_{effect} involves stronger VEP responses to IC presence than absence, with an onset as early as ~90ms post-stimulus and sources within bilateral lateral occipital cortices (Murray et al, 2002; reviewed in Murray and Herrmann, 2013). The IC_{effect} is robust to myriad differences in the kinds of stimuli used to induce perceptions of illusory contours (i.e. the particular shape induced, the contrast polarity of the stimuli/background, the types of inducers, whether or not modal or amodal completion is induced, the chromaticity of the inducers, and the parafoveal spatial eccentricity of the inducers) as well as whether or not participants perform a task or even correctly perceive the IC shape (Anken et al., 2016; reviewed in Murray and Herrmann, 2013).

A further model contends that LOC are sensitive to salient regions defined by inducers and that IC sensitivity happens in V1/V2 only after feedback modulation from the LOC (Stanley and Rubin, 2003; Yoshino et al., 2006). However, positive evidence of modulated responses within V1/V2 is critically missing in the results reported by Stanley and Rubin (2003). It thus remains unknown to what extent regions V1/V2 exhibit illusory contour sensitivity in humans. Evidence supporting the necessary, albeit perhaps pre-attentive, role of LOC in illusory contour sensitivity comes from neuropsychological reports in brain-lesions individuals. Perceptual benefits of illusory contours on a line bisection task were observed only when LOC were intact, but not when lesioned (Vuilleumier et al., 2001). In all cases, areas V1/V2 were intact and there was no evidence of lesions or anopia.

Nonetheless, embracing any of these models is complicated, in part, by a lack of temporal information regarding neurophysiologic effects, variability in the stimuli employed, as well as by any contributions of inter-species differences in brain mechanisms of IC sensitivity. Unfortunately, temporal information on precisely when post-stimulus time histograms of neural firing rates differed

across stimulus conditions were not reported nor evident in the figures in the overwhelming majority of electrophysiological studies of IC processes in animals. To the best of our knowledge, the first study reporting temporal dynamics in such work was Lee and Nguyen (2001). This study reported both the timing of effects as well as their laminar origin. They found that effects in areas V1 and V2 in the macaque were consistent with feedback inputs originating outside of V2. The earliest effects were at ~70ms in superficial layers of V2, followed by effects in deep layers of V2 at 95ms and in superficial layers of V1 at 100ms, with the latest effects in deep layers of V1 at ~120ms. In addition, Sàry et al. (2007) provided evidence for sensitivity to illusory contours of complex shapes peaking at ~120ms within inferotemporal cortices. Applying a 3:5 ratio for comparison of timing in macaques vs. humans (Musacchia and Schroeder, 2009), would estimate the peak of comparable effects in humans at ~170ms.

Demonstrations of the IC_{effect} in humans typically used inducers that spanned across several degrees of visual angle as well as across either/both the vertical or horizontal meridians of the visual field (e.g. 6° in Murray et al., 2002; see also **Figure 1a**). Consequently, it can reasonably be argued that feedforward processing of ICs in brain areas such as V1/V2 would be favoured in human subjects if the stimuli induce illusory lines rather than geometric forms, and also when the induced contour spans relatively short distances that match the small receptive fields observed in V1/V2. Some studies have partially addressed these points in humans by positioning inducing stimuli within a single visual hemifield (Brandeis and Lehmann, 1989; Murray et al., 2002; Senkowski et al., 2005) or by parametrically varying the eccentricity of the inducers or the support ratio of the bound IC form (and by extension the distance to be perceptually completed;(Altschuler et al., 2012). Such manipulations resulted in *delayed* $IC_{effects}$, which is contrary to expectations if IC sensitivity is a strictly feedforward process in V1/V2.

In light of these collective discrepancies, here we presented participants with illusory contour lines while measuring VEPs and the IC_{effect}. Our objective was to emulate stimulation conditions similar to those used in the seminal work in non-human primates by von der Heydt, Peterhans, and their

colleagues (von der Heydt et al., 1984), thereby facilitating the reconciliation of discrepant findings across species and stimulus parameters. As detailed below, the stimuli used here are highly similar in terms of their form, overall size of inducers, and the relative size of the illusory contour and notch inducers to the stimuli used in Peterhans and von der Heydt (1989) (**Figure 1**). We reasoned that centrally presented and small illusory contour lines would favour visual completion processes within lower-tier visual cortices (V1/V2), if indeed V1/V2 are required for IC sensitivity in humans. Specifically, we hypothesized that if IC sensitivity is indeed mediated by feedforward processes in V1/V2 then the IC_{effect} in response to illusory contour lines would be earlier than that characterized in our (and others') prior works that presented relatively large IC shapes. That is, the simpler form of a line vs. geometric shape as well as smaller distances required for visual completion should lead to faster neural IC sensitivity. Likewise, an IC_{effect} mediated by feedforward processes within V1/V2 would not be predicted to be affected by other surrounding inducer stimuli that fail to form illusory contours. This is because any neural responses to these other inducers should be treated independently of those to inducers resulting in an illusory contour (e.g. Kapadia et al., 1999 suggest that the horizontal connections within V1/V2 extend ~2° in macaque monkeys). For this reason, stimulus arrays used in the present study consisted of multiple inducer stimuli; although only a pair of which could result in an illusory contour on any trial. In terms of the IC_{effect}, the prediction would be that it is contemporaneous with VEP onset (i.e. at ~50ms; (Foxe and Simpson, 2002; Murray et al., 2001)). By contrast, IC sensitivity at latencies ≥90ms post-stimulus and with localization within LOC would be consistent with a potentially size-invariant mechanism within higher-level visual cortices (Dura-Bernal et al., 2011; Mendola et al., 1999; Murray et al., 2002).

2. Materials and Methods

2.1. Participants

Analyses presented in this study are based on data from 11 participants (6 male, all right-handed; aged 23-36years, mean 27.7 years). No subject had a history of or current neurological or

psychiatric illnesses. All participants had normal or corrected-to normal vision. Data from an additional 3 subjects, beyond the 11 reported here, were excluded due to either technical issues with behavioural response recording during data acquisition (N = 1) or excessive muscle and/or alpha frequency EEG artefacts (N = 2). All participants provided written, informed consent to procedures approved by the cantonal ethics committee.

2.2. Stimuli and task

Stimuli were comprised of a set of 10 circular Kanizsa-type (Kanizsa, 1976) 'pacmen' inducers that were arranged in an array (**Figure 1d**). The size of the array was 4.87° wide x 1.86° high, each inducer subtended 0.57° in diameter, and the induced illusory contour line was 1.50° in length from a distance of 80cm. Illusory contour lines could be oriented, when present, either horizontally or vertically with equal likelihood. Stimuli were displayed on a LCD computer monitor (20" active TFT, 1600 x 1200 @ 60Hz, 16ms pixel response time). On a given trial, two of the ten inducers were positioned with their mouths facing each other to create an illusory contour line that was presented either centrally or laterally (left, right). Alternatively and with equal likelihood, no inducers were facing each other to create a no contour (NC) equivalent. These variations in the presentation of ICs were included to prevent participants from selectively focusing on a particular region of space or on any single inducer as a strategy to successfully complete the task. However, we focus our analyses here on the centrally-presented ICs. Each participant completed 10 blocks of trials. Each block contained 160 stimuli with equivalent probability of apparition of vertical and horizontal IC in one location and NC conditions. Stimuli were presented for 500ms with an inter-stimulus interval ranging between 800 and 1200ms with a uniform distribution. A white central fixation cross was displayed on the computer screen during the inter-stimulus interval. During the experiment, participants took regular breaks between blocks to maintain high concentration and prevent fatigue.

Participants performed a four-alternative forced choice that required indicating the presence vs. absence of an illusory contour and, if judged present, whether the IC was positioned in the left, center, or right. All participants answered with their right hand. Responses were given with the index

finger (left IC), middle finger (central IC), ring finger (right IC), and small finger (NC). Accuracy and reaction time were measured with a serial response box (Psychology Software Tools; https://www.pstnet.com/hardware.cfm?ID=102). Stimulus delivery and behavioural response collection were controlled with PsychoPy (Peirce, 2007; Peirce and Peirce, 2009).

2.3. EEG acquisition and pre-processing

Continuous EEG was acquired at 1024Hz through a 128-channel Biosemi ActiveTwo AD-box (http://www.biosemi.com) referenced to the common mode sense (CMS; active electrode) and grounded to the driven right leg (DRL; passive electrode), which functions as a feedback loop driving the average potential across the electrode montage to the amplifier zero (full details, including a diagram of this circuitry, can be found at http://www.biosemi.com/faq/cms&drl.htm). Prior to epoching, the continuous EEG was filtered (0.1Hz high-pass; 60Hz low-pass; 50Hz notch). The filters were computed linearly in both forward and backward directions to eliminate phase shifts.

EEG epochs were time-locked to the visual presentation of stimuli and spanned 100ms pre-stimulus to 800ms post-stimulus. Epochs with amplitude deviations over ±80μV at any channel, with the exception of electrodes with poor electrode-skin contact or damage labelled as 'bad', were considered artefacts and were excluded. Eye blinks were also excluded off-line based on vertical and horizontal electro-oculograms. After averaging, channels labelled as 'bad' were interpolated using 3D splines (Perrin et al., 1987). This allowed for the same number of channels from each participant/condition and for proper calculation of the average reference. Data from the visual evoked potential (VEP) were baseline-corrected using the pre-stimulus interval and re-calculated against an average reference. For each participant, 2 VEPs were calculated: IC in the Center (ICC) and No contour (NCC). The mean number of accepted EEG epochs (±s.e.m.) for each of these conditions was 189±3 and 190±3 out of a maximum of 266 for these conditions, avoiding issues of unequal signal-to-noise across conditions (e.g. (Files et al., 2016) for discussion).

2.4. VEP analyses

VEP analyses were performed with both the Cartool freeware (http://sites.google.com/site/fbmlab/cartool/cartooldownload; (Brunet et al., 2011) and statistical as well as STEN utilities developed by Jean-François Knebel and Michael Notter (http://doi.org/10.5281/zenodo.1164038). An electrical neuroimaging analysis framework identified effects (Koenig et al., 2014; Michel et al., 2004; Michel and Murray, 2012; Murray et al., 2008; Tzovara et al., 2012). These analyses differentiate between effects due to modulations in VEP response strength, latency, or topography. Our VEP analyses focused on identifying brain mechanisms underlying the detection of centrally-presented illusory contour lines and therefore contrasted ICC vs. NCC. The Supplementary Materials report results of a 2×3 ANOVA on the IC_{effect} as a function of line position (left, center, and right) as well as orientation (horizontal vs. vertical). Because the main effect of IC line position as well as the interaction between factors were at latencies equal to or later than what we report below of the centrally-presented stimuli, we do not discuss the results in fuller detail in the main text. There was no main effect of the orientation of the IC line.

For the contrast of the ICC and NCC responses, we first performed a mass univariate test (each electrode as a function of peri-stimulus time). This was included here primarily for illustrative purposes, given the well-known effect of the choice of the reference on statistical analyses of voltage waveforms (c.f. (Murray et al., 2008) for discussion). It also is included here to facilitate comparison with works displaying voltage waveforms and to facilitate comprehension of the results for readers less familiar with measures such as global field power or global dissimilarity.

In terms of the electrical neuroimaging framework, we first statistically compared the Global Field Power (GFP), which quantifies the electric field at the scalp level (Lehmann and Skrandies, 1980). This measure of the VEP strength is equivalent to the root mean square of the voltage potential values of electrodes at a given time point and is calculated versus the average reference ((Koenig et al., 2014; Koenig and Melie-García, 2010; Murray et al., 2008); though see also ((Yao, 2017)) for discussion of the average reference). Global Dissimilarity (DISS) was then analysed in order to test for changes in the VEP topography independently of its strength (Lehmann and Skrandies, 1980). DISS is equivalent to

the square root of the mean of the squared difference between the potentials measured at each electrode for different conditions, normalized by the instantaneous GFP. This measure is directly related to the (spatial) correlation between two normalized vectors (cf. Appendix in (Murray et al., 2008). The DISS was used in an analysis called "TANOVA" (Murray et al., 2008). In the "TANOVA", the DISS value at each time point is compared to an empirical distribution derived from permuting the condition label of the data from each subject. As changes in VEP topographies at the scalp forcibly reflect changes in the configuration of active generators in the brain (Lehmann et al., 1987), this analysis indicates if distinct brain networks are involved in IC sensitivity and/or during brain discrimination of the orientation of ICs. Additionally, a topographic cluster analysis based on a hierarchical clustering algorithm (Murray et al., 2008) was performed on the group-average VEPs. This clustering analysis identifies stable VEP topographies across time in the group-averaged data after first strength-normalizing the data (hereafter template maps). In this way, this clustering is sensitive exclusively to topographic modulations within and between conditions. The optimal number of template maps (i.e. the minimal number of maps that accounts for the greatest variance of the dataset) was determined using a modified Krzanowski-Lai criterion (Murray et al., 2008). Template maps identified in the group-averaged VEP were then submitted to a fitting procedure in which each time point of each single-subject VEP from each condition was labelled according to the template map with which it best correlated spatially (Murray et al., 2008).This procedure allows for statistically testing the relative presence of each template map across time of the single-subject VEPs; and therefore the differences across conditions. These values can be expressed as the probability of a given template map yielding a higher spatial correlation in the single-subject data from each condition. Statistical analysis of these values was performed with the Wilcoxon signed-rank test.

2.5. Source Estimations

Finally, we estimated the intracranial sources using a distributed linear inverse solution (ELECTRA) together with the local autoregressive average (LAURA) regularization approach to address the non-uniqueness of the inverse problem (Grave de Peralta Menendez et al., 2001; Grave De Peralta

Menendez et al., 2004; Michel et al., 2004). This inverse solution algorithm is based on biophysical principles derived from the quasi-stationary Maxwell's equations; most notably the fact that independent of the volume conductor model used to describe the head, only irrotational and not solenoidal currents contribute to the EEG (Grave de Peralta Menendez et al., 2001; Grave De Peralta Menendez et al., 2004). As part of the LAURA regularization strategy, homogenous regression coefficients in all directions and within the whole solution space were used. The solution space includes 3005 nodes, distributed within the grey matter of the Montreal Neurological Institute's average brain (courtesy of Dr. Rolando Grave de Peralta Menendez and Dr. Sara Gonzalez Andino). The head model and lead field matrix were generated with the Spherical Model with Anatomical Constraints (SMAC;(Spinelli et al., 2000) as implemented in Cartool. As an output, LAURA provides current density measures; the scalar values of which were evaluated at each node. Prior basic and clinical research has documented and discussed in detail the spatial accuracy of this inverse solution (Gonzalez Andino et al., 2005; Grave De Peralta Menendez et al., 2004; Martuzzi et al., 2009). The relevant time interval for source estimation was determined based on the above topographic clustering analysis to identify periods of temporally-stable VEP topography. Data were first averaged across time for each subject and condition, and then source estimations were calculated based on these time-averaged data. These data matrices were then contrasted using a paired t-test. To partially correct for multiple testing we applied a significance threshold of $p<0.05$ at each solution point as well as a spatial-extent criterion (k_E) of >15 contiguous solution points (Bourquin et al., 2013; De Lucia et al., 2010; Knebel and Murray, 2012; Matusz et al., 2015; Toepel et al., 2015).

3. Results

Accuracy rates for all conditions were between 96-98%, mean 97%. These values provide a clear indication that all conditions were visible and readily perceived. There were no reliable differences between ICC and NCC ($t_{(10)} = 0.52$; $p>0.05$). Analyses of reaction times indicated faster

responses for the presence than absence of illusory contours (ICC vs. NCC: 589±17ms vs. 688±20ms; $t_{(10)} = 8.95, p<0.01$).

Figure 2a displays VEPs in response to the ICC and NCC conditions at an exemplar midline occipital scalp site (Oz). Both ICC and NC elicited robust VEPs with characteristic P1-N1 components of indistinguishable magnitude**.** In order to identify the timing of differential VEP responses, we first performed a mass univariate analysis as a function of time across the full 128-channel electrode montage (**Figure 2b**). To (partially) account for both temporal and spatial correlation, differences were considered reliable if significant for at least 15ms consecutively (i.e. >15 time samples) as well as across at least 20% of the electrode montage (i.e. >25 electrodes; green line in **Figure 2b**). Reliable differences began at 189ms post-stimulus onset. Next, analyses were performed using reference-independent and global measures of the brain's electric field at the scalp. The first of these was the global field power (GFP), which exhibited significant differences between responses to ICC and NCC over the 416-456ms post-stimulus period. Responses were significantly stronger to the ICC than NCC condition. Analysis of the VEP topography, using global dissimilarity, indicated that responses to ICC and NCC first differed topographically over the 181-334ms post-stimulus interval with additional differences during subsequent post-stimulus intervals (**Figure 2d**).

In order to better understand the nature of these topographic differences, the group-averaged ICC and NCC data were submitted to a topographic cluster analysis. Two template maps were identified to be present over the 212-319 ms post-stimulus period in the group-averaged data. These template maps were then fitted to the single-subject ICC and NCC VEPs to determine the relative presence of each map over the 212-319ms period in each subject's data. These values were then submitted to a Wilcoxon Signed-Ranks Test, which indicated a significant interaction $Z=21$, $p <0.05$. One map predominated responses to ICC, whereas another map predominated responses to NCC (**Figure 2e**). Finally, analyses were performed using distributed source estimations from the 212-319ms period (i.e. the period identified in the above topographic clustering analysis). **Figure 2f** displays the statistical differences between group-averaged source estimations in response to ICC and NCC conditions.

Significantly stronger source estimations were observed in response to the ICC condition within the left LOC and extending to the ventral occipito-temporal cortex.

4. Discussion

This study addressed a major discrepancy across prior investigations of the neural mechanisms subserving illusory contour sensitivity in humans and animals; namely whether or not this sensitivity unfolds in a strictly feedforward manner. This discrepancy was hitherto exacerbated by the fact that while many studies in animals presented small and central stimuli resulting in illusory contour lines, all prior studies in humans had presented comparatively large, bilateral stimuli resulting in illusory contour forms or shapes. By presenting illusory contour lines to humans and recording VEPs, we addressed this discrepancy and showed that a strictly feedforward model of IC sensitivity within V1/V2 is untenable. Rather, IC sensitivity appears to rely first on processes within LOC.

The timing of the IC_{effect} was delayed and onset at ~200ms when presenting participants with IC lines, in contrast to the onset at ~90ms in prior works involving presentation of IC shapes (Murray and Herrmann, 2013). Two temporally distinct stages of perceptual completion have been previously distinguished. The first, considered to be largely automatic or at least invariant to task demands and performance outcome, onsets at ~90ms and peaks at ~150ms. This is the IC_{effect} that our laboratory and many others have repeatedly characterised, which has been reliably observed independently of multiple variations in the low-level features and types of stimuli presented (reviewed in Murray and Herrmann, 2013; see also Anken et al., 2016 and Tivadar et al., 2018). The second stage of perceptual completion is considered to reflect a shift to a more effortful or conceptual mode of perceptual completion (e.g. (Altschuler et al., 2012; Doniger et al., 2001; Humphreys et al., 2000; Murray et al., 2002; Ritter et al., 1982; Tulving and Schacter, 1990)). This stage has been characterized by a VEP modulation referred to as the closure negativity or N_{cl} (Doniger et al., 2000). The N_{cl} has been shown to track the perceptual completion of fragmented images, with an onset at ~220ms post-stimulus

onset, peak at ~300ms, and bilateral LOC localisation (Sehatpour et al., 2008, 2006). These temporal stages have moreover been dissociated in patients with schizophrenia as well as 22q11.2DS patients, in whom the IC_{effect} appears to be intact (Biria et al., 2018; Foxe et al., 2005; Knebel et al., 2011) whereas the N_{cl} is severely impaired (Doniger et al., 2002).

The relatively protracted timing of IC sensitivity we observed here was also accompanied by significant topographic VEP modulations between responses to ICC and NCC over the 212-319ms post-stimulus period (Figures 2d and 2e). IC sensitivity occurring during the period of the IC_{effect} consistently manifests as a modulation in VEP strength in the absence of modulations in VEP topography (Knebel and Murray, 2012; Murray et al., 2006, 2004; Pegna et al., 2002), whereas, studies reporting IC sensitivity during the N_{cl} stage have instead reliably observed topographic VEP modulations between contour present and absent conditions (Brandeis and Lehmann, 1989; Shpaner et al., 2009; Yoshino et al., 2006). The present results are thus in strong agreement with this pattern, wherein IC sensitivity during the later N_{cl} stage follows from changes in VEP topography, rather than strength. Topographic modulations forcibly reflect differences in the configuration of the underlying sources active in the brain (Lehmann et al., 1987). Statistical analyses of source estimations localized effects within the left LOC and ventral occipito-temporal cortices, which are regions repeatedly shown to be involved both in IC sensitivity as well as perceptual completion. An important question for future research will be to disentangle whether the present effect at 200ms represents a delayed version of the IC_{effect} typically observed at 90ms, constitutes an N_{cl}, or instead is an entirely distinct process. Use of the present stimulus paradigm with some of the abovementioned clinical populations may be a way to address this, if it is indeed the case that the N_{cl} is impaired in patients with chronic schizophrenia whereas the IC_{effect} remains intact.

Another (the first one being that it represents the N_{cl} instead of the IC_{effect}) possible explanation for this shifted timing and topographic vs. strength-based mechanism is visual crowding. In other words, the timing of the IC sensitivity we observed here was a consequence of the number of inducers presented on a given trial, many of which did not result in the formation or perception of an IC line.

The complexity of the visual context in which illusory contours appear may be a (partial) determinant of the timing of IC sensitivity. Two studies from separate laboratories argue against this possibility. On the one hand, Senkowski et al. (2005) showed that visual search performance was unaffected by increasing stimulus set sizes; i.e. RTs increased with a slope below 10ms per item in the stimulus set. On the other hand, Halgren et al. (Halgren et al., 2003) observed an IC_{effect} with a peak latency of 155ms within LOC despite presenting a large array of 56 inducers on each trial in the absence of task requirements beyond the maintenance of central fixation (cf. their Figure 1). If the number of inducers were strongly influencing the timing of IC sensitivity, then a delayed effect relative to that observed with substantially fewer inducers would have been expected. This was not the case.

It might also be argued that the uncertainty of the spatial location of the illusory contours is the determinant of the latency of VEP correlates of IC sensitivity. That is, in our study the IC lines, when present, could appear with equal probability at any of three locations (centrally, left, and right) and two orientations (horizontal and vertical). Participants were thus required to divide their attention accordingly; albeit limited spatially to the central 5° for the whole array of 10 inducers. This might perhaps account for differences between an IC_{effect} at ~90ms vs. ~200ms, and by extension the shift from a perceptual to conceptual mode of visual completion (cf. (Altschuler et al., 2014; Doniger et al., 2001; Foxe et al., 2005)). The same shift in time to a later IC_{effect} has been reported previously in Experiment 5 of Murray et al. (2002). In their study stimulus arrays were limited to one or the other visual hemifield on any trial (though spatially unpredictable across trials). Similarly, in Experiment 2 of Senkowski et al. (2005) stimulus arrays consisted of 23 bilaterally-distributed inducers and IC shapes were presented on 67% of trials to either the left or right visual hemifield (see also Brandeis and Lehmann, 1989). However, this uncertainty of the spatial location of the IC would fail to explain why the IC_{effect} did not shift earlier in time if indeed IC sensitivity were under the control of a strictly feedforward mechanism as some data in animals would have predicted. When considered alongside the published literature, uncertainty regarding spatial location, even when limited to the central 5°, seems to be a more likely factor than the degree of crowding in the visual stimulus array (e.g. (Gebodh

et al., 2017; Hansen et al., 2016) for discussion). Undoubtedly, continued research will be necessary to assess this proposition in a more controlled, parametric manner.

On the one hand, our results provide additional insight regarding the determinants of the timing of neural sensitivity to illusory contours. Perhaps more critically, our results also help to address the knowledge gap between how IC sensitivity has been studied in humans versus animal models. Part of this knowledge gap stemmed from brain imaging and mapping studies in humans having used illusory contour forms exclusively, whereas many studies in animals used stimuli forming illusory contour lines. We therefore presented our participants with stimuli highly similar in form and size (both overall and in terms of the illusory line) to those previously used in studies in animal models. The timing and localization of IC sensitivity to these stimuli contribute to the accumulation of evidence favouring a model of IC sensitivity that relies first on processes within LOC with effects in V1/V2 driven by feedback inputs (Murray and Herrmann, 2013).

5. Acknowledgements

The Swiss National Science Foundation (grants 320030-149982 and 320030-169206), the Swiss Brain League (2014 Research Prize), the Fondation Asile des Aveugles (SEER project; grant 232933), and a grantor advised by Carigest SA provided financial support to MMM. The authors have no conflicts of interest to disclose. J.A. and M.M.M. designed the study. J.A. and J.F.K. collected and analysed data. R.I.T. performed analyses during the revision process. J.A., R.I.T and M.M.M. wrote and revised the manuscript. All authors provided written feedback on the manuscript.

6. References

Altschuler, T.S., Molholm, S., Butler, J.S., Mercier, M.R., Brandwein, A.B., Foxe, J.J., 2014. The effort to close the gap: tracking the development of illusory contour processing from childhood to adulthood with high-density electrical mapping. Neuroimage 90, 360–73. https://doi.org/10.1016/j.neuroimage.2013.12.029

Altschuler, T.S., Molholm, S., Russo, N.N., Snyder, A.C., Brandwein, A.B., Blanco, D., Foxe, J.J., 2012. Early electrophysiological indices of illusory contour processing within the lateral occipital complex are virtually impervious to manipulations of illusion strength. Neuroimage 59, 4074–85. https://doi.org/10.1016/j.neuroimage.2011.10.051

Anken, J., Knebel, J., Crottaz-herbette, S., Matusz, P.J., Lefebvre, J., Murray, M.M., 2016. Cue-dependent circuits for illusory contours in humans. Neuroimage 129, 335–344. https://doi.org/10.1016/j.neuroimage.2016.01.052

Biria, M., Tomescu, M.I., Custo, A., Cantonas, L.M., Song, K.-W., Schneider, M., Murray, M.M., Eliez, S., Michel, C.M., Rihs, T.A., 2018. Visual processing deficits in 22q11.2 Deletion Syndrome. NeuroImage Clin. 17, 976–986. https://doi.org/10.1016/j.nicl.2017.12.028

Bourquin, N.M.-P., Murray, M.M., Clarke, S., 2013. Location-independent and location-linked representations of sound objects. Neuroimage 73, 40–9. https://doi.org/10.1016/j.neuroimage.2013.01.026

Brandeis, D., Lehmann, D., 1989. Segments of event-related potential map series reveal landscape changes with visual attention and subjective contours. Electroencephalogr. Clin. Neurophysiol. 73, 507–19.

Brunet, D., Murray, M.M., Michel, C.M., 2011. Spatiotemporal analysis of multichannel EEG: CARTOOL. Comput. Intell. Neurosci. 2011, 813870. https://doi.org/10.1155/2011/813870

De Lucia, M., Michel, C.M., Murray, M.M., 2010. Comparing ICA-based and single-trial topographic ERP analyses. Brain Topogr. 23, 119–127. https://doi.org/10.1007/s10548-010-0145-y

Doniger, G.M., Foxe, J.J., Murray, M.M., Higgins, B. a, Snodgrass, J.G., Schroeder, C.E., Javitt, D.C., 2000. Activation timecourse of ventral visual stream object-recognition areas: high density electrical mapping of perceptual closure processes. J. Cogn. Neurosci. 12, 615–21.

Doniger, G.M., Foxe, J.J., Murray, M.M., Higgins, B.A., Javitt, D.C., 2002. Impaired Visual Object Recognition and Dorsal/Ventral Stream Interaction in Schizophrenia. Arch Gen Psychiatry 59, 1011–1020. https://doi.org/10.1001/archpsyc.59.11.1011

Doniger, G.M., Foxe, J.J., Schroeder, C.E., Murray, M.M., Higgins, B. a, Javitt, D.C., 2001. Visual perceptual learning in human object recognition areas: a repetition priming study using high-density electrical mapping. Neuroimage 13, 305–13. https://doi.org/10.1006/nimg.2000.0684

Dura-Bernal, S., Wennekers, T., Denham, S.L., 2011. The role of feedback in a hierarchical model of object perception. Adv. Exp. Med. Biol. 718, 165–79. https://doi.org/10.1007/978-1-4614-0164-3_14

Files, B.T., Lawhern, V.J., Ries, A.J., Marathe, A.R., 2016. A Permutation Test for Unbalanced Paired Comparisons of Global Field Power. Brain Topogr. 29, 345–357. https://doi.org/10.1007/s10548-016-0477-3

Foxe, J.J., Murray, M.M., Javitt, D.C., 2005. Filling-in in schizophrenia: a high-density electrical mapping and source-analysis investigation of illusory contour processing. Cereb. Cortex 15, 1914–27. https://doi.org/10.1093/cercor/bhi069

Foxe, J.J., Simpson, G. V, 2002. Flow of activation from V1 to frontal cortex in humans. A framework for defining “early” visual processing. Exp. Brain Res. 142, 139–50. https://doi.org/10.1007/s00221-001-0906-7

Gebodh, N., Vanegas, M.I., Kelly, S.P., 2017. Effects of Stimulus Size and Contrast on the Initial Primary Visual Cortical Response in Humans. Brain Topogr. 30, 450–460. https://doi.org/10.1007/s10548-016-0530-2

Gonzalez Andino, S.L., Michel, C.M., Thut, G., Landis, T., De Peralta, R.G., 2005. Prediction of response

speed by anticipatory high-frequency (gamma band) oscillations in the human brain. Hum. Brain Mapp. 24, 50–58. https://doi.org/10.1002/hbm.20056
Grave de Peralta Menendez, R., Gonzalez Andino, S., Lantz, G., Michel, C.M., Landis, T., 2001. Noninvasive localization of electromagnetic epileptic activity. I. Method descriptions and simulations. Brain Topogr. 14, 131–7.
Grave De Peralta Menendez, R., Murray, M.M., Michel, C.M., Martuzzi, R., Gonzalez Andino, S.L., 2004. Electrical neuroimaging based on biophysical constraints. Neuroimage 21, 527–539. https://doi.org/10.1016/j.neuroimage.2003.09.051
Grosof, D.H., Shapley, R.M., Hawken, M.J., 1993. Macaque V1 neurons can signal "illusory" contours. Nature 365, 550–552. https://doi.org/10.1038/365550a0
Halgren, E., Mendola, J., Chong, C.D.., Dale, A.M., 2003. Cortical activation to illusory shapes as measured with magnetoencephalography. Neuroimage 18, 1001–1009. https://doi.org/10.1016/S1053-8119(03)00045-4
Hansen, B.C., Haun, A.M., Johnson, A.P., Ellemberg, D., 2016. On the Differentiation of Foveal and Peripheral Early Visual Evoked Potentials. Brain Topogr. 29, 506–514. https://doi.org/10.1007/s10548-016-0475-5
Humphreys, G.W., Cinel, C., Wolfe, J., Olson, a, Klempen, N., 2000. Fractionating the binding process: neuropsychological evidence distinguishing binding of form from binding of surface features. Vision Res. 40, 1569–96.
Kanizsa, G., 1976. Subjective contours. Sci. Am. 234, 48–52.
Knebel, J.-F., Javitt, D.C., Murray, M.M., 2011. Impaired early visual response modulations to spatial information in chronic schizophrenia. Psychiatry Res. 193, 168–76. https://doi.org/10.1016/j.pscychresns.2011.02.006
Knebel, J.-F., Murray, M.M., 2012. Towards a resolution of conflicting models of illusory contour processing in humans. Neuroimage 59, 2808–17. https://doi.org/10.1016/j.neuroimage.2011.09.031
Koenig, T., Melie-García, L., 2010. A method to determine the presence of averaged event-related fields using randomization tests. Brain Topogr. 23, 233–242. https://doi.org/10.1007/s10548-010-0142-1
Koenig, T., Stein, M., Grieder, M., Kottlow, M., 2014. A tutorial on data-driven methods for statistically assessing ERP topographies. Brain Topogr. 27, 72–83. https://doi.org/10.1007/s10548-013-0310-1
Lee, T.S., Nguyen, M., 2001. Dynamics of subjective contour formation in the early visual cortex. Proc. Natl. Acad. Sci. U. S. A. 98, 1907–1911.
Lehmann, D., Ozaki, H., Pal, I., 1987. EEG alpha map series: brain micro-states by space-oriented adaptive segmentation. Electroencephalogr. Clin. Neurophysiol. 67, 271–288.
Lehmann, D., Skrandies, W., 1980. Reference-free identification of components of checkerboard-evoked multichannel potential fields. Electroencephalogr. Clin. Neurophysiol. 48, 609–621.
Martuzzi, R., Murray, M.M., Meuli, R. a, Thiran, J.-P., Maeder, P.P., Michel, C.M., Grave de Peralta Menendez, R., Gonzalez Andino, S.L., 2009. Methods for determining frequency- and region-dependent relationships between estimated LFPs and BOLD responses in humans. J. Neurophysiol. 101, 491–502. https://doi.org/10.1152/jn.90335.2008
Matusz, P.J., Thelen, A., Amrein, S., Geiser, E., Anken, J., Murray, M.M., 2015. The role of auditory cortices in the retrieval of single-trial auditory-visual object memories. Eur. J. Neurosci. 41, 699–708. https://doi.org/10.1111/ejn.12804
Mendola, J.D., Dale, a M., Fischl, B., Liu, a K., Tootell, R.B., 1999. The representation of illusory and real contours in human cortical visual areas revealed by functional magnetic resonance imaging. J. Neurosci. 19, 8560–72.
Michel, C.M., Murray, M.M., 2012. Towards the utilization of EEG as a brain imaging tool. Neuroimage 61, 371–85. https://doi.org/10.1016/j.neuroimage.2011.12.039
Michel, C.M., Murray, M.M., Lantz, G., Gonzalez, S., Spinelli, L., Grave de Peralta, R., 2004. EEG source imaging. Clin. Neurophysiol. Off. J. Int. Fed. Clin. Neurophysiol. 115, 2195–2222.

https://doi.org/10.1016/j.clinph.2004.06.001
Murray, M.M., Brunet, D., Michel, C.M., 2008. Topographic ERP analyses: a step-by-step tutorial review. Brain Topogr. 20, 249–64. https://doi.org/10.1007/s10548-008-0054-5
Murray, M.M., Foxe, D.M., Javitt, D.C., Foxe, J.J., 2004. Setting boundaries: brain dynamics of modal and amodal illusory shape completion in humans. J. Neurosci. 24, 6898–903. https://doi.org/10.1523/JNEUROSCI.1996-04.2004
Murray, M.M., Foxe, J.J., Higgins, B. a, Javitt, D.C., Schroeder, C.E., 2001. Visuo-spatial neural response interactions in early cortical processing during a simple reaction time task: a high-density electrical mapping study. Neuropsychologia 39, 828–44.
Murray, M.M., Herrmann, C.S., 2013. Illusory contours: A window onto the neurophysiology of constructing perception. Trends Cogn. Sci. https://doi.org/10.1016/j.tics.2013.07.004
Murray, M.M., Imber, M.L., Javitt, D.C., Foxe, J.J., 2006. Boundary completion is automatic and dissociable from shape discrimination. J. Neurosci. 26, 12043–54. https://doi.org/10.1523/JNEUROSCI.3225-06.2006
Murray, M.M., Wylie, G.R., Higgins, B. a, Javitt, D.C., Schroeder, C.E., Foxe, J.J., 2002. The spatiotemporal dynamics of illusory contour processing: combined high-density electrical mapping, source analysis, and functional magnetic resonance imaging. J. Neurosci. 22, 5055–73.
Musacchia, G., Schroeder, C.E., 2009. Neuronal mechanisms, response dynamics and perceptual functions of multisensory interactions in auditory cortex. Hear. Res. 258, 72–9. https://doi.org/10.1016/j.heares.2009.06.018
Nieder, a, Wagner, H., 1999. Perception and neuronal coding of subjective contours in the owl. Nat. Neurosci. 2, 660–3. https://doi.org/10.1038/10217
Pegna, A.J., Khateb, A., Murray, M.M., Landis, T., Michel, C.M., 2002. Neural processing of illusory and real contours revealed by high-density ERP mapping. Neuroreport 13, 965–8.
Peirce, J.W., 2007. PsychoPy—Psychophysics software in Python. J. Neurosci. Methods 162, 8–13. https://doi.org/10.1016/j.jneumeth.2006.11.017
Peirce, J.W., Peirce, J.W., 2009. Generating stimuli for neuroscience using PsychoPy. Front. Neuroinform. 2, 10. https://doi.org/10.3389/neuro.11.010.2008
Poscoliero, T., Girelli, M., 2017. Electrophysiological Modulation in an Effort to Complete Illusory Figures: Configuration, Illusory Contour and Closure Effects. Brain Topogr. 0, 0. https://doi.org/10.1007/s10548-017-0582-y
Redies, C., Crook, J.M., Creutzfeldt, O.D., 1986. Neuronal responses to borders with and without luminance gradients in cat visual cortex and dorsal lateral geniculate nucleus. Exp. Brain Res. 61, 469–81.
Ritter, W., Simson, R., Vaughan, H.G., Macht, M., 1982. Manipulation of event-related potential manifestations of information processing stages. Science 218, 909–911.
Sáry, G., Chadaide, Z., Tompa, T., Köteles, K., Kovács, G., Benedek, G., 2007. Illusory shape representation in the monkey inferior temporal cortex. Eur. J. Neurosci. 25, 2558–64. https://doi.org/10.1111/j.1460-9568.2007.05494.x
Sáry, G., Köteles, K., Kaposvári, P., Lenti, L., Csifcsák, G., Frankó, E., Benedek, G., Tompa, T., 2008. The representation of Kanizsa illusory contours in the monkey inferior temporal cortex. Eur. J. Neurosci. 28, 2137–46. https://doi.org/10.1111/j.1460-9568.2008.06499.x
Sehatpour, P., Molholm, S., Javitt, D.C., Foxe, J.J., 2006. Spatiotemporal dynamics of human object recognition processing: An integrated high-density electrical mapping and functional imaging study of “closure” processes. Neuroimage 29, 605–618. https://doi.org/10.1016/j.neuroimage.2005.07.049
Sehatpour, P., Molholm, S., Schwartz, T.H., Mahoney, J.R., Mehta, A.D., Javitt, D.C., Stanton, P.K., Foxe, J.J., 2008. A human intracranial study of long-range oscillatory coherence across a frontal – occipital – hippocampal brain network during visual object processing PSYCHOLOGY.
Senkowski, D., Röttger, S., Grimm, S., Foxe, J.J., Herrmann, C.S., 2005. Kanizsa subjective figures capture visual spatial attention: evidence from electrophysiological and behavioral data. Neuropsychologia 43, 872–86. https://doi.org/10.1016/j.neuropsychologia.2004.09.010

Shpaner, M., Murray, M.M., Foxe, J.J., 2009. Early processing in the human lateral occipital complex is highly responsive to illusory contours but not to salient regions. Eur. J. Neurosci. 30, 2018–28. https://doi.org/10.1111/j.1460-9568.2009.06981.x

Spinelli, L., Andino, S.G., Lantz, G., Seeck, M., Michel, C.M., 2000. Electromagnetic inverse solutions in anatomically constrained spherical head models. Brain Topogr. 13, 115–25.

Stanley, D. a, Rubin, N., 2003. fMRI activation in response to illusory contours and salient regions in the human lateral occipital complex. Neuron 37, 323–31.

Tivadar, R.I., Retsa, C., Turoman, N., Matusz, P.J., Murray, M.M., 2018. Sounds enhance visual completion processes. Neuroimage. https://doi.org/10.1016/j.neuroimage.2018.06.070

Toepel, U., Bielser, M.-L., Forde, C., Martin, N., Voirin, A., le Coutre, J., Murray, M.M., Hudry, J., 2015. Brain dynamics of meal size selection in humans. Neuroimage 113, 133–142. https://doi.org/10.1016/j.neuroimage.2015.03.041

Tulving, E., Schacter, D.L., 1990. Priming and human memory systems. Science 247, 301–306.

Tzovara, A., Murray, M.M., Michel, C.M., De Lucia, M., 2012. A tutorial review of electrical neuroimaging from group-average to single-trial event-related potentials. Dev. Neuropsychol. 37, 518–44. https://doi.org/10.1080/87565641.2011.636851

Ungerleider, L.G., Mishkin, M., 1982. Two cortical visual systems, in: Visual Behavior. D.J. Ingle, M.A. Goodale & R.J.W. Mansfield, pp. 549–586.

von der Heydt, R., Peterhans, E., Baumgartner, G., 1984. Illusory contours and cortical neuron responses. Science 224, 1260–1262.

Vuilleumier, P., Valenza, N., Landis, T., 2001. Explicit and implicit perception of illusory contours in unilateral spatial neglect: behavioural and anatomical correlates of preattentive grouping mechanisms. Neuropsychologia 39, 597–610.

Yao, D., 2017. Is the Surface Potential Integral of a Dipole in a Volume Conductor Always Zero? A Cloud Over the Average Reference of EEG and ERP. Brain Topogr. 30, 161–171. https://doi.org/10.1007/s10548-016-0543-x

Yoshino, A., Kawamoto, M., Yoshida, T., Kobayashi, N., Shigemura, J., Takahashi, Y., Nomura, S., 2006. Activation time course of responses to illusory contours and salient region: a high-density electrical mapping comparison. Brain Res. 1071, 137–44. https://doi.org/10.1016/j.brainres.2005.11.089

Figure Captions

Figure 1. Examples of illusory contours. **a.** The pacemen inducers are oriented to give the impression of a complete square. This stimulus, popularized by Gaetano Kanisza has been used in many studies of IC processes in humans, e.g. Murray et al., 2002 where the illusory square measured 6 degrees on each side. **b.** An example is displayed of an illusory contour line induced by phase-shifted gratings. Such stimuli have been used in single-unit electrophysiologic studies in animals (e.g. Redies et al., 1986; von der Heydt and Peterhans, 1989). **c.** The notch stimuli used by Peterhans and von der Heydt (1989) are displayed. The red arrows indicate that the stimulus array was moved across the display. The dotted oval indicates the approximate receptive field of the neurons from which their recordings were made. It should be noted that the notch stimuli were located outside of the receptive field and resulted in an illusory contour spanning ~2° of visual angle. **d.** Exemplar inducer stimulus array used in the present study and its spacing. The array consisted of 10 circular inducers presented within the parafovea (central ~5° of visual angle). In this example, 2 inducers were oriented to result in the perception of a central, horizontal line measuring 1.5° of visual angle. Note that stimuli are shown here as black on white, whereas the contrast polarity during the experiment was reversed (i.e. white inducers on a black background). Full details are provided in Materials and Methods.

Figure 2. VEP correlates of sensitivity to IC lines as revealed by the electrical neuroimaging analysis framework. **a.** Group-averaged (N=11) VEPs in response to the ICC and NCC conditions at an exemplar midline occipital scalp site (Oz) are displayed. **b.** The results of a mass univariate analysis as a function of time across the full 128-channel electrode montage show differences starting at 189ms post-stimulus onset. The 20% threshold is indicated by the green line. **c.** The group-averaged global field power (GFP) waveforms from the ICC and NCC conditions are displayed. **d.** The analysis of VEP topography based on global dissimilarity showed that ICC and NCC first differed topographically over the 181-334ms post-stimulus with additional subsequent effects over the majority of the post-stimulus period. **e.** The group-averaged ICC and NCC responses were submitted to a topographic cluster

analysis. Two template maps were identified over the 212-319ms post-stimulus time period (top view and back view are shown). These maps were fitted to the single-subject data from each condition using spatial correlation. The percentage of this time window when each map better correlated spatially with each condition is shown in the bar graph (mean±s.e.m. displayed). Different maps significantly better characterised responses to each condition. **f.** Statistical differences between group-averaged distributed source estimations in response to ICC and NCC conditions were observed within the left LOC and extending to the ventral occipito-temporal cortex. Only effects with $p<0.05$ and extending across at least 15 contiguous nodes ($k_E>15$) were considered reliable.

Graphical Abstract

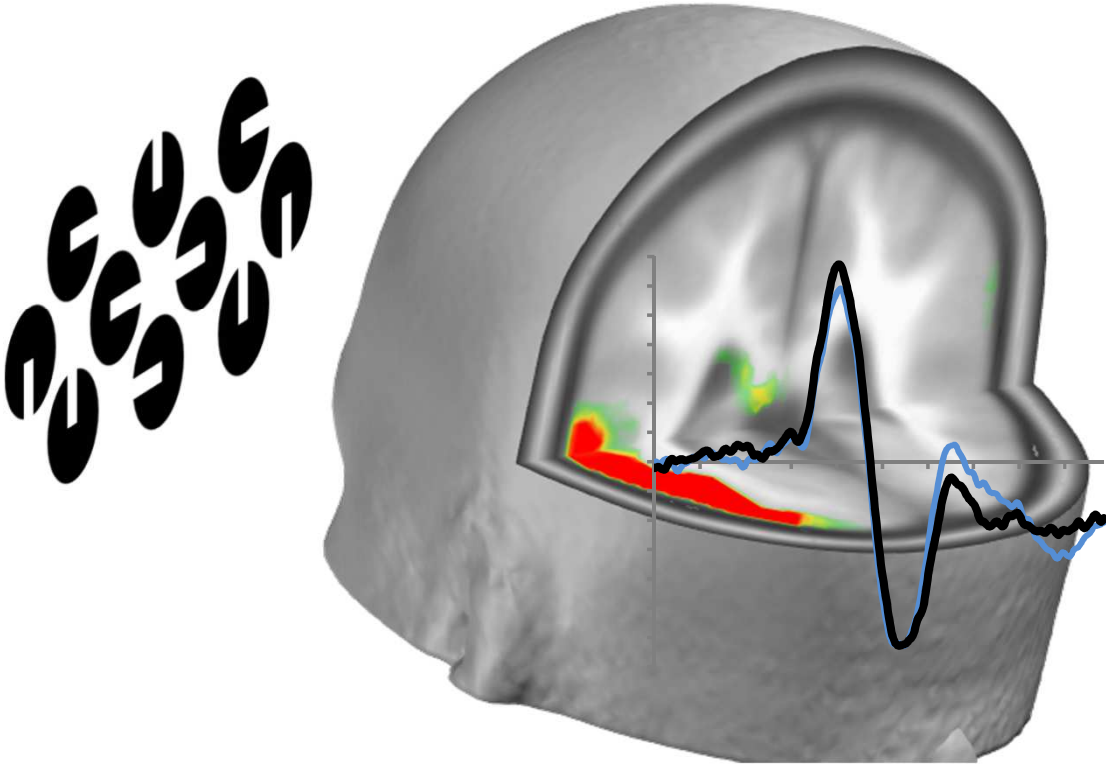

Figure 1

a.

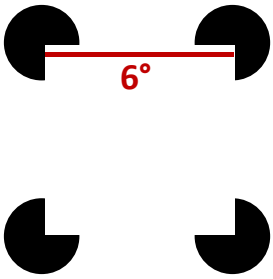

b.

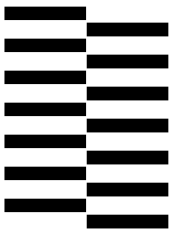

c.

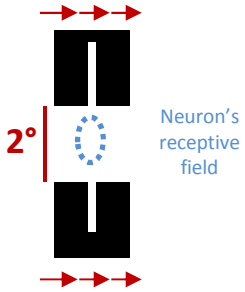

d.

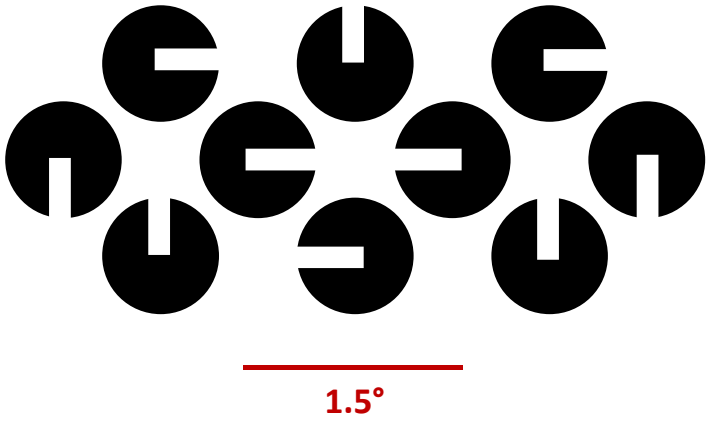

Figure 2

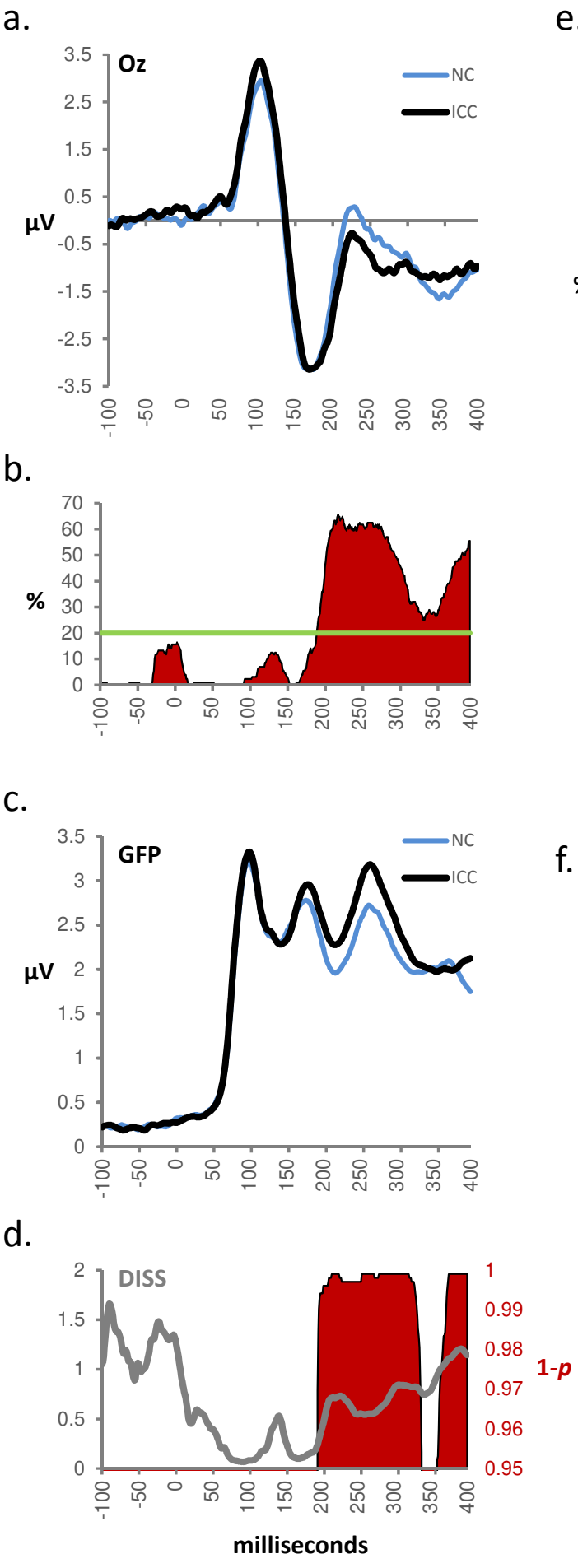
a.
Oz
NC
ICC
µV
3.5
2.5
1.5
0.5
-0.5
-1.5
-2.5
-3.5
-100
-50
0
50
100
150
200
250
300
350
400
b.
%
70
60
50
40
30
20
10
0
c.
GFP
NC
ICC
µV
3.5
3
2.5
2
1.5
1
0.5
0
d.
DISS
2
1.5
1
0.5
0
1
0.99
0.98
0.97
0.96
0.95
1-p
milliseconds
e.
NC
ICC
%
90
80
70
60
50
40
30
20
10
0
top
back
f.
p<0.05; k_E>15nodes

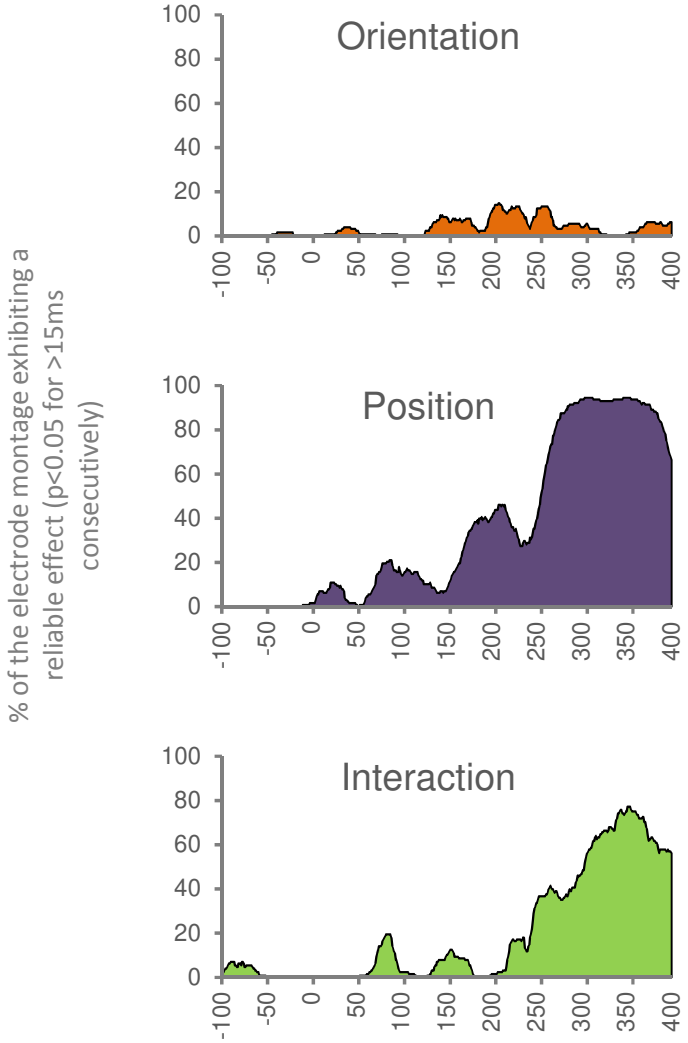

Supplementary Figure S1. Analyses of VEP waveform data on the IC effect resulting from the subtraction of responses to NC from those to IC conditions. These analyses followed a 2x3 (IC orientation x IC position) factorial design. There was no evidence of a reliable main effect of IC orientation (vertical vs. horizontal). There was a reliable main effect of IC position as well as an interaction between factors. Note that both were only at latencies equal to or later than that observed for the contrast of ICC vs. NC reported in the main text.